Bias and Variability of Diagnostic Spectral Parameters Extracted from Closing Sounds Produced by Bioprosthetic Valves Implanted in the Mitral Position

GUY CLOUTIER, STUDENT MEMBER, IEEE, LOUIS-GILLES DURAND, SENIOR MEMBER, IEEE, ROBERT GUARDO, HANI N. SABBAH, AND PAUL D. STEIN

Abstract—**A method is proposed to estimate the bias and variability of eight diagnostic spectral parameters extracted from mitral closing sounds produced by bioprosthetic heart valves. These spectral parameters are: the frequency of the dominant ($F1$) and second dominant ($F2$) spectral peaks, the highest frequency of the spectrum found at -3 dB (F-3), -10 dB (F-10) and -20 dB (F-20) below the highest peak, the relative integrated area above -20 dB of the dominant peak (RIA20), the bandwidth at -3 dB of the dominant spectral peak (BW3), and the ratio of $F1$ divided by BW3 ($Q1$). The bias and variability of four spectral techniques were obtained by comparing parameters extracted from each technique with the parameters of a spectral "standard." This "standard" consisted of 19 normal mitral sound spectra computed analytically by evaluating the Z transform of a sum of decaying sinusoids on the unit circle. Truncation of the synthesized mitral signals and addition of random noise were used to simulate the physiological characteristics of the closing sounds. Results show that the fast Fourier transform method with rectangular window provides the best estimates of $F1$ and $Q1$, that the Steiglitz-McBride method with maximum entropy (pole-zero modeling with four poles and four zeros) can best evaluate $F2$, F-20, RIA20 and BW3, and that the all-pole modeling with covariance method (16 poles) is best suited to compute F-3. It was also shown that both the all-pole modeling and the Steiglitz-McBride methods can be used to estimate F-10. It is concluded that a single algorithm would not provide the best estimates of all spectral parameters.**

I. Introduction

A. Selection of the Mitral Component (M1) of the First Heart Sound (S1)

According to Shaver *et al.* [1], Tilkian and Boudreau Conover [2], and Leatham [3], the first heart sound $S1$ is composed of two major transient waves, $M1$ and $T1$, which are related, respectively, to the closure of the mitral and tricuspid heart valves. Normally, $T1$ follows $M1$ and the duration of normal $S1$ ranges between 100 and 120 ms [2], [4]. The normal splitting interval between $M1$ and $T1$ depends largely on the recording site of the phonocardiogram (PCG). Leatham [3] reported a splitting interval ranging between 20 and 30 ms for PCG's recorded at the lower left sternal edge. No apparent splitting interval was found between $M1$ and $T1$ for PCG's recorded at the apex [2].

To study closing sounds produced by bioprosthetic heart valves implanted in the mitral position, only the $M1$ component of $S1$ is of interest. However, the selection of the mitral component may be difficult because $M1$ and $T1$ are often merged together. Transient waves such as ejection sounds of stenotic aortic valves [1], [2], [5] and opening clicks of prosthetic aortic valves [6], appearing close to $S1$ and often superimposed on $T1$, also increase the difficulty in selecting $M1$. For this reason, most investigators have used the entire first heart sound to assess mitral heart valve dysfunctions by the spectral analysis of the phonocardiogram. In the present paper, extraction of $M1$ will be performed by a semi-automatic method previously developed to select aortic heart sound components from the second heart sound [7], [8].

B. Spectral Analysis of M1 and S1

Detection of mitral valve diseases by the spectral analysis of $S1$ has gained in acceptance since the early 1980's. The work of Stein *et al.* [9], [10] has largely contributed to increase the diagnostic utility of this technique. Their studies on natural and porcine bioprosthetic valves have clearly demonstrated that the dominant spectral peak ($F1$) of $S1$ shifts towards the higher frequencies as a result of calcification, fibrosis, and stiffening. Recently, Durand *et al.* [11] have described a pattern recognition algorithm based on nine spectral diagnostic features for detecting the degeneration of aortic and mitral bioprosthetic valves. Correct classification seemed promising with the use of multiple spectral diagnostic features, and the use of additional spectral features is being explored.

A statistical analysis was performed by Arnott *et al.* [12] on a group of normal and hypertensive patients to

Manuscript received June 28, 1988; revised January 26, 1989. This work was supported in part by the Natural Sciences and Engineering Council of Canada and the Canadian Heart Foundation.

G. Cloutier and L.-G. Durand are with the Biomedical Engineering Laboratory, Clinical Research Institute of Montreal and Biomedical Engineering Institute, Ecole Polytechnique, University of Montreal, Quebec, Canada.

R. Guardo is with the Biomedical Engineering Institute, Ecole Polytechnique, University of Montreal, Quebec, Canada.

H. N. Sabbah and P. D. Stein are with the Department of Medicine, Division of Cardiovascular Medicine and Department of Surgery, Henry Ford Hospital, Detroit, MI.

0018-9294/89/0800-0815$01.00 © 1989 IEEE

relate sex, blood pressure, and body surface area with the frequency content of normal first and second ($S2$) heart sounds. The values of $F1$, extracted from the spectra of $S1$ and $S2$, appeared to be unrelated to any of these parameters. They have shown, however, that the high frequency content of $S1$ (above 160 Hz) decreases as body surface increases and systolic pressure decreases.

Recently, Cloutier *et al.* [13] and Durand *et al.* [8] have shown that changes in background noise and signal duration of aortic closing sounds can affect the accuracy of FFT-based and parametric methods in estimating diagnostic spectral parameters. Stein *et al.* [9], [10] and Durand *et al.* [11] used the fast Fourier transform with rectangular window and Arnott *et al.* [12] used the fast Fourier transform with Hamming window to estimate these parameters. No other spectral techniques were tested in these studies. In spite of the promising results reported by Durand *et al.* [11], other investigations are needed to better characterize the effect of background noise and signal truncation on the extraction of spectral features from mitral heart sounds.

C. Outline of the Paper

The objective of the present paper is to evaluate the bias and variability of various spectral estimation techniques in the extraction of diagnostic spectral parameters used to detect valvular degeneration. In this paper, we evaluated the difference between the parameters extracted from closing sound spectra using various algorithms and the parameters obtained from a reliable "standard." This "standard" was synthesized by adding a series of exponentially decaying sinusoids, and is used solely to evaluate the performance of the tested spectral algorithms. The "standard" spectrum was computed analytically by evaluating the Z transform of the synthesized signals on the unit circle. Addition of random noise and truncation of the synthesized sounds were then used to assess the accuracy of the various methods in estimating eight diagnostic spectral parameters. The results obtained suggest that the utilization of the optimal spectral technique for each parameter should provide diagnostic features having better discriminant properties.

II. Materials and Methods

A. Data Acquisition

A group of 19 patients with normal functioning Ionescu–Shiley bioprosthetic valves implanted in the mitral position was selected from subjects in postoperative follow-up and in the early recovery period. The valve status was assessed by clinical history and was considered "normal" when the subject had no symptom or auscultatory sign of valve degeneration or malfunction.

For each patient, the electrocardiogram (ECG) and phonocardiogram were recorded with a multichannel FM recorder having a bandwidth of 0–2500 Hz. The PCG was captured with a Hewlett-Packard contact microphone (no. 21050A) placed at the apex, while the patient was in a supine position. Prior to recording, the PCG was preprocessed by a third-order high-pass filter (18 dB/octave) with a cutoff frequency of 100 Hz. This high-pass filter is used for: 1) emphasizing the acoustic components of the precordial vibrations, 2) compensating the attenuation slope of the heart sounds, and 3) maximizing the signal-to-noise ratio of the PCG. At playback, the PCG was low-pass filtered at 900 Hz with an eight-order filter (-48 dB/octave) to prevent frequency aliasing. The ECG and PCG were then digitized with 12-bit resolution at sampling rates of 250 and 2500 Hz, respectively.

The beginning of each cardiac cycle was automatically identified by a *QRS* detection algorithm applied to the ECG. A typical mitral closing sound was chosen manually by moving a window on the PCG and saved as a reference closing sound. The Q waves of the ECG were then used to synchronize the selection of $M1$. Time alignment with the reference mitral sound was done automatically by a correlation technique and an ensemble average of 20 mitral closing sounds was computed for each patient to estimate the acoustic signature of the mitral valve.

This semi-automatic heart sound selection procedure was previously used by our group to extract the aortic component of $S2$ from digitized PCG [7], [8]. The main advantages of this approach are the exclusion of undesirable transient sounds such as $T1$ and the increase of the signal-to-noise ratio (SNR) of $M1$. However, this technique truncates the portion of $M1$ superimposed on $T1$.

B. Synthesis of Mitral Heart Sounds

For each patient studied, a synthesized bioprosthetic mitral closing sound was established by adding a series of exponentially decaying sinusoids of variable amplitude, frequency, damping, and phase. More precisely, each acoustic mitral signature $s(n)$ was modeled by

$$\hat{s}(n) = \sum_{i=1}^{R} A(i)\, e^{-n/\tau(i)} \sin\left(n\omega(i) + \psi(i)\right) \qquad n \geq 0 \tag{1}$$

where

$\hat{s}(n)$ = synthesized mitral acoustic signature
R = number of decaying sinusoids
$A(i)$ = amplitude of the ith sinusoid
$\tau(i)$ = decay time constant of the ith sinusoid (s)
$\omega(i)$ = frequency of the ith sinusoid (rad/s)
$\psi(i)$ = phase of the ith sinusoid (rad).

Valve closing sounds were synthesized as follows [7], [14]. First, the FFT power spectrum of the valve closing sound to be synthesized was computed. *A priori* knowledge of the duration of $M1$ was used to choose the decay time constant of the synthesized sound. From this spectrum, the relative amplitude and frequency location of the dominant peak were used as first estimates for the parameters of the first decaying sinusoid ($R = 1$). Phase values of 0 and π radians were used as initial estimates. Then, the FFT power spectrum of the synthesized sound was evaluated after truncating the signal to the same duration as the valve sound and computing its root-mean-square (rms) value. The synthesized and valve closing sound spectra were normalized with respect to their rms values, compared, and the parameters readjusted to obtain a closer fit. Depending on the morphology of the valve closing sound being synthesized, other decaying sinusoids were added. The three last steps of this interactive procedure, involving the parameter adjustment and the spectral comparison, were repeated until the synthesized sound matched the valve sound within a level of precision determined by the four criteria described next.

Another group has recently proposed a different approach for modeling mitral heart sounds with a series of exponentially decaying cosinusoids [15]. Their method is based on the recursive implementation of Prony's method for estimating the parameters of (1). The required number of decaying cosinusoids was estimated with the Levinson–Durbin order selection method. Both Prony's and Levinson–Durbin's methods are described in the review paper of Kay and Marple [16].

In our paper, the synthesized sounds were considered to be representative of the real mitral sounds only if the following criteria were met:

1) The maximal value of the correlation function between the acoustic signature of a given mitral valve and the corresponding synthesized sound was greater than 98 percent.

2) The normalized root-mean-square error (NRMSE),[1] found at maximum correlation, was less than 20 percent.

3) The envelope of the synthesized sound was such that 95 percent of the sound energy was contained in the first 50 ms segment.

4) 99 percent of the energy was contained in the first 75 ms segment.

The percentage of sound energy was obtained by dividing the sound energy of the 50 and 75 ms segments with the energy of the synthesized sound computed over a duration of 120 ms. The last two criteria are used to ensure that the duration of the synthesized sounds was in accordance with information published in the literature.

The power spectra of the synthesized sounds $\hat{s}(n)$, used as a "gold standard" in this analysis, were computed analytically by evaluating the Z transform of $\hat{s}(n)$ on the unit circle.

$$\hat{S}_{ss}(Z) = \hat{S}_{ss}(e^{jW}) = \left| \sum_{i=1}^{R} A(i) \frac{N}{D} \right|^2 \qquad (2)$$

where the numerator

$$N = e^{2jW} \sin(\psi(i)) + e^{((-1/\tau(i))+jW)} \cdot \sin(\omega(i) - \psi(i)),$$

and the denominator

$$D = e^{2jW} - 2e^{((-1/\tau(i))+jW)} \cos(\omega(i)) + e^{-2/\tau(i)}.$$

[1]$\text{NRMSE} = \left| \sum_{n=0}^{N-1} (s(n) - \hat{s}(n))^2 \right|^{1/2} \Big/ \left| \sum_{n=0}^{N-1} s(n)^2 \right|^{1/2}.$

Although an infinite resolution characterized the synthesized spectra, the computation was done by dividing the unit circle into 1024 samples to obtain the same number of samples as those used in the spectral algorithms evaluated (FFT-based and parametric algorithms).

C. Spectral Analysis of the Mitral Sounds

Four algorithms of spectral estimation were tested to extract eight diagnostic spectral features from the synthesized mitral sounds after truncation and noise contamination. The algorithms were: a) the fast Fourier transform with rectangular (FFTR) and b) Hamming (FFTM) windows, c) the Steiglitz–McBride method with maximum entropy (SMME) [17], [18], and d) the all-pole modeling with covariance method (APC) [19], [20].

The number of poles (P) and zeros (Q) for parametric modeling was evaluated by computing, for different values of P and Q, the normalized root-mean-square error (NRMSE) function between the real mitral acoustic signature of each patient and the impulse response of SMME and APC. The NRMSE was computed at maximal correlation of the signals and on the interval corresponding to the duration of the mitral acoustic signatures. Optimal values of P and Q were then chosen at the point marking the beginning of the plateau of the NRMSE curve [21].

This procedure represents a compromise between the criterion proposed by Childers [22] and that reported by Joo [23]. Other criteria, based on the statistical properties and the autocorrelation function of modeled zero mean random signals, have also been proposed. Among these, the Akaike criteria are widely used [24], [25]. However, these criteria have not been used in our analysis mostly because the acoustic closing sounds are not random signals but transient signals.

An additional test was performed to ensure that the chosen values of P and Q minimized the bias and variability of the spectral parameters. For instance, spectra of the 19 synthesized mitral sounds were computed with SMME and APC following truncation and noise contamination. Bias and variability measurements were then evaluated for different values of P and Q and compared to the results obtained by using the values estimated from the NRMSE function.

D. Extraction of the Spectral Parameters

Eight spectral parameters, initially proposed by Durand *et al.* [11], were extracted from each spectrum. These parameters, shown in Fig. 1, are as follows:

a) $F1$: the frequency of the dominant spectral peak (Hz),

b) $F2$: the frequency of the second dominant spectral peak (Hz),

c) F-3: the highest frequency found at -3 dB below the dominant spectral peak (Hz),

d) F-10: the highest frequency found at -10 dB below the dominant spectral peak (Hz),

e) F-20: the highest frequency found at -20 dB below the dominant spectral peak (Hz),

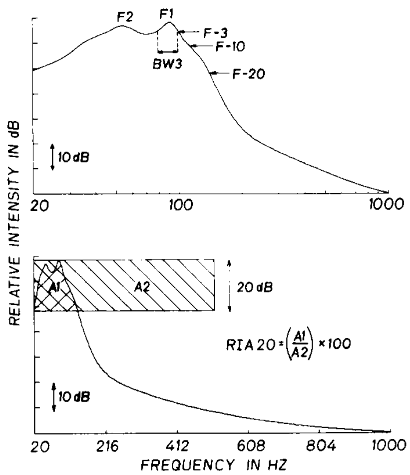

Fig. 1. Description of the spectral parameters $F1$, $F2$, F-3, F-10, F-20, RIA20, and BW3. Parameter $Q1$ is computed by dividing $F1$ by BW3.

f) RIA20: the relative integrated area above -20 dB of the dominant spectral peak (percent),

g) BW3: the bandwidth at -3 dB of the dominant spectral peak (Hz),

h) $Q1$: the ratio of $F1$ divided by BW3.

The following criteria were imposed for the estimation of the spectral parameters. First, search of the spectral peaks and computation of RIA20 were limited to the frequency band of 20–500 Hz. These boundaries were used to minimize the sidelobe effects of FFTR and spurious production of false spectral peaks by the APC and SMME algorithms. For instance, appearance of spurious details was reported when using the maximum entropy spectral algorithms with a high-order model [16], [22], [26] or a low SNR [27]. In addition, Steiglitz and McBride [17] and Joo [23] reported that the high-order pole-zero algorithms tend to model the noise, thus exhibiting spurious peaks on the spectrum.

A peak detection algorithm was used as a second criterion to differentiate an inflection on the spectrum from a true peak. This was done by centering a window over each potential peak and accepting it as a true peak only if at least two samples (4.9 Hz) before and after it were of lower intensity. Finally, to prevent noise from appearing as the second dominant peak, all peaks with an intensity of -35 dB lower than that of $F1$ were rejected.

Additional constraints were utilized for the extraction of the spectral parameters. The estimation of the highest frequencies found at -3, -10, and -20 dB was confined to frequencies between $F1$ and 600 Hz. The parameter RIA20, expressed in percent, was related to a rectangle having a height of 20 dB and a length of 480 Hz on a linear scale. Finally, if a minimum was found before the amplitude of the dominant peak had decreased by -3 dB, the frequency of this minimum was used in computing BW3.

E. Bias and Variability of the Spectral Parameters

The "reference" values of the spectral parameters were computed from the synthesized spectra. As described previously, these spectra were computed by evaluating the Z transform, on the unit circle, of the synthesized sounds untruncated and uncontaminated by random noise. Then, the spectral parameters were extracted from the FFTR, FFTM, APC, and SMME algorithms after truncating the synthesized sounds and adding random noise. Computation of the bias and variability of a given spectral algorithm was done by comparing the "reference" values of the spectral parameters with those extracted with the tested algorithms, by using each patient synthesized closing sound spectrum as its own reference. Details concerning the computation of the bias and variability of the spectral parameters are described next.

For each patient, the bias of a given algorithm was computed individually by subtracting the value of the "reference" parameter, from the value of the same parameter estimated with the tested algorithm. The sign of this difference indicated the direction of the bias. The variability of the tested algorithms was evaluated, for each patient, by computing the absolute difference between the parameters extracted from the synthesized spectrum and those estimated with FFTR, FFTM, APC, or SMME spectra. The variability of an algorithm was always greater than or equal to its bias. Bias and variability measurements were finally average over the 19 patients. These mean values were used to characterize the bias and variability of each spectral algorithms.

F. Estimation of the Truncation Level and SNR of the Mitral Sounds

In a previous analysis, we have proposed a method to estimate the truncation level and signal-to-noise ratio of aortic closing sounds [7]. A similar approach has been used in this paper to estimate these two characteristics of mitral acoustic signatures.

The information on $M1$ that was lost during coherent detection and averaging of $M1$ was computed from the synthesized sounds using

$$\text{percent of truncation} = 100 - \left(\left(E(M1)/E(SM1)\right) \times 100\right) \quad (3)$$

where $E(M1)$ is the energy of the synthesized sound computed on the interval corresponding to the duration of the real mitral acoustic signature and $E(SM1)$ is the energy of the entire synthesized sound computed on an interval of 120 ms (see Fig. 2). This procedure is justified by the fact that the decay rate of the synthesized sounds was chosen to match that of the real mitral closing sounds.

The signal-to-noise ratio of the mitral sounds was estimated by repeating the data acquisition with the same QRS detection algorithm. However, the 19 PCG's analyzed were extended by 200 ms before the onset of $M1$

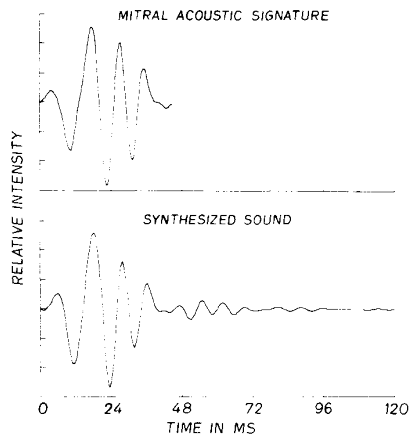

Fig. 2. Comparison of a synthesized sound with the corresponding mitral signature of a patient with a Ionescu–Shiley bioprosthetic heart valve. A correlation level of 98.1 percent and a normalized rms error of 19.4 percent were obtained between these signals.

with a portion of the diastolic phase. For each patient, 20 PCG segments as well as an ensemble average were saved for further analysis.

Assuming that the background noise in the selected normal PCG's was stationary and that no diastolic murmur or significant fourth heart sound occurred in the extended 200 ms segment before $S1$, the *SNR* of the mitral sounds was estimated by

$$SNR = 10 \log \left(\left(E(M1) - E(N) \right) / E(N) \right) \quad (4)$$

where $E(M1)$ is the energy of the mitral component of duration M, and $E(N)$ the energy of the background noise computed during the diastolic phase by using the first M samples of the extended PCG segments. Two measurements of the *SNR* ratio were taken from each PCG: the mean SNR of $M1$ (averaged from the 20 PCG segments of each patient) and the mean SNR of the mitral acoustic signature obtained from the mean PCG segment of each patient.

G. Perturbation of the Synthesized Mitral Sounds

Normal mitral closing sounds are characterized by a patient to patient variation in SNR and duration of $M1$. The effects of adding random noise and truncating the synthesized mitral sounds, on the accuracy of the spectral algorithms, were investigated by adding various levels (-45, -35, and -25 dB) of random noise and by truncating the signals. Truncation levels of 2, 6, and 10 percent of the signal energy, computed over a duration of 120 ms, were tested.

III. Results

The mitral acoustic signatures obtained by coherent averaging were characterized by a duration of 32 ± 12 ms (mean $\pm$ standard deviation). The minimum and maximum durations of $M1$ were 18.8 and 50.8 ms, respectively. The durations of the corresponding synthesized sounds after truncation by 2, 6, and 10 percent of their total energy were, respectively, 42 ± 11 ms (range of 14.8–68.0 ms), 30 ± 8 ms (range of 10.8–48.8 ms), and 25 ± 6 ms (range of 9.6–34.8 ms). A mean correlation level of 99.0 ± 0.5 percent (range of 98.1–99.8 percent) and a mean NRMSE of 14 ± 4 percent (range of 6–19 percent) were obtained between the synthesized sounds and the acoustic signatures of $M1$. These performances were achieved by summing between 3 and 12 decaying sinusoids in the synthesis process [parameter R of (1)].

The percentages of total energy found in the synthesized sounds during the first 50 and 75 ms segments were 99 ± 1 percent (range of 95–100 percent) and 99.9 ± 0.1 percent (range of 99.4–100 percent), respectively. These results indicate that the decay rate of the synthesized sounds was similar to that of the real valve closing sounds. Fig. 2 presents a comparison of a synthesized sound with the corresponding mitral signature of a patient with a Ionescu–Shiley bioprosthetic heart valve.

A. Truncation Level and SNR of M1

The mean energy of the part of $M1$ truncated by the *QRS* detection algorithm was 6 ± 4 percent (range of 0.4–13 percent). The mean SNR of the mitral sounds, estimated by averaging the SNR of 20 PCG segments for each patient, was 24 ± 7 dB (range of 15–38 dB). The mean SNR of the acoustic mitral signature of each patient, computed from the averaged PCG segments, was 35 ± 7 dB (range of 26–45 dB). This result proves the effectiveness of coherent averaging for improving the SNR of $M1$. Indeed, a mean increase in the SNR by 11 dB was obtained.

B. Number of Poles and Zeros for the APC and SMME Algorithms

The averaged NRMSE functions for the 19 patients are shown in Fig. 3 for APC and SMME. No plateau but a minimum was observed on the NRMSE curve computed with APC. The optimal number of poles for modeling normal mitral acoustic signatures with the all-pole algorithm and covariance method was found to be 16. This value corresponds to the minimum of the NRMSE curve computed for P (number of poles) varying from 4 to 24. For the pole-zero Steiglitz–McBride method, the NRMSE function was evaluated for Q (number of zeros) $= P$ where P varied from 6 to 24. A first plateau was found at $P = Q = 8$ and a second at $P = Q = 20$. The optimal number of poles and zeros was chosen at 20 because it corresponds to the beginning of the plateau with the lowest values of the NRMSE.

An additional analysis was performed with the synthesized mitral sounds to ensure that the selected values of P and Q minimized the bias and variability of the spectral parameters. Synthesized mitral sounds truncated by 6 percent of their energy and contaminated by -35 dB of random noise were used to test the effect of varying P and

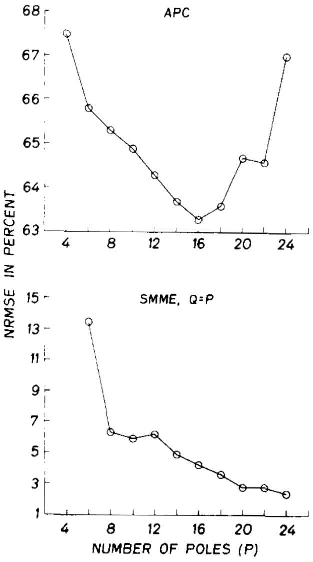

Fig. 3. Average normalized root-mean-square error (NRMSE) as a function of the number of poles (P). NRMSE was computed between the mitral acoustic signatures and the impulse responses of the all-pole model with covariance method (APC) and the Steiglitz–McBride method with maximum entropy (SMME). The number of zeros (Q) used for SMME was equal to the value of P.

TABLE I

BIAS (B) AND VARIABILITY (V) OF THE ALL-POLE MODELING WITH COVARIANCE METHOD (APC) FOR DIFFERENT VALUES OF THE NUMBER OF POLES (P). B AND V ARE ESTIMATED FOR THE EIGHT DIAGNOSTIC SPECTRAL PARAMETERS AFTER TRUNCATING THE SYNTHESIZED SOUNDS BY 6 PERCENT OF THEIR ENERGY AND AFTER ADDING −35 dB OF RANDOM NOISE

	P = 8	P = 12	P = 16
F1 (Hz)	B = 7.3 V = 12.3	B = 1.9 V = 13.5	B = -3.6 V = 11.1
F2 (Hz)	B = 288.2 V = 295.5	B = 241.8 V = 261.6	B = 158.0 V = 179.8
F-3 (Hz)	B = 21.0 V = 23.0	B = 6.8 V = 14.3	B = 0.4 V = 11.6
F-10 (Hz)	B = 30.5 V = 34.9	B = 11.2 V = 24.9	B = 5.0 V = 19.2
F-20 (Hz)	B = 157.8 V = 157.8	B = 135.6 V = 135.9	B = 141.7 V = 148.9
RIA20 (%)	B = 8.1 V = 8.3	B = 3.2 V = 5.7	B = 2.1 V = 4.6
BW3 (Hz)	B = 41.5 V = 42.3	B = 20.1 V = 30.6	B = 12.2 V = 23.7
Q1	B = -2.1 V = 2.2	B = -0.1 V = 3.4	B = -0.4 V = 2.9

natures.

Table I presents the results obtained with APC by varying P from 8 to 16. Results for lower values of P were not shown because the resulting spectra appeared to be oversmoothed and no second dominant spectral peak could be observed. Results for values of P higher than 16 were also rejected because of the occurrence of false spectral peaks and because no benefit was observed in Fig. 3 when increasing P over 16. Except for F-20 and $Q1$, P equals to 16 always resulted in a minimum of the variability of the spectral parameters. The bias also decreased progressively for $F2$, F-3, F-10, RIA20, and BW3 when P increased up to 16. For this reason, the optimal value of the number of poles was kept at 16 for modeling mitral heart sounds with APC.

TABLE II

BIAS (B) AND VARIABILITY (V) OF THE STEIGLITZ–MCBRIDE METHOD WITH MAXIMUM ENTROPY (SMME) FOR DIFFERENT VALUES OF THE NUMBER OF POLES (P) AND THE NUMBER OF ZEROS (Q). B AND V ARE ESTIMATED FOR THE EIGHT DIAGNOSTIC SPECTRAL PARAMETERS AFTER TRUNCATING THE SYNTHESIZED SOUNDS BY 6 PERCENT OF THEIR ENERGY AND AFTER ADDING −35 dB OF RANDOM NOISE

	P = Q 4	P = Q 8	P = Q 12	P = Q 16	P = Q 20
F1 (Hz)	B = 1.8 V = 12.5	B = -2.7 V = 12.9	B = -7.1 V = 14.9	B = -7.4 V = 13.3	B = -8.3 V = 12.5
F2 (Hz)	B = -2.5 V = 25.2	B = 28.6 V = 38.4	B = 64.2 V = 73.9	B = 65.8 V = 79.6	B = 82.7 V = 97.5
F-3 (Hz)	B = -4.0 V = 17.1	B = 3.1 V = 14.9	B = 1.7 V = 17.7	B = 3.5 V = 13.1	B = 0.1 V = 16.2
F-10 (Hz)	B = -15.6 V = 20.4	B = 14.4 V = 26.0	B = 15.5 V = 37.2	B = 7.9 V = 21.6	B = 9.1 V = 18.8
F-20 (Hz)	B = -9.2 V = 24.0	B = 49.9 V = 65.5	B = 116.2 V = 127.5	B = 113.8 V = 124.4	B = 123.1 V = 140.7
RIA20 (%)	B = -1.5 V = 3.7	B = 1.8 V = 5.6	B = 2.5 V = 6.0	B = 2.8 V = 5.7	B = 2.3 V = 5.7
BW3 (Hz)	B = -4.5 V = 15.5	B = 7.0 V = 23.1	B = 12.3 V = 26.2	B = 12.5 V = 25.0	B = 13.3 V = 26.3
Q1	B = 3.2 V = 4.2	B = 2.0 V = 4.7	B = 0.5 V = 3.6	B = 0.6 V = 3.9	B = 0.7 V = 3.8

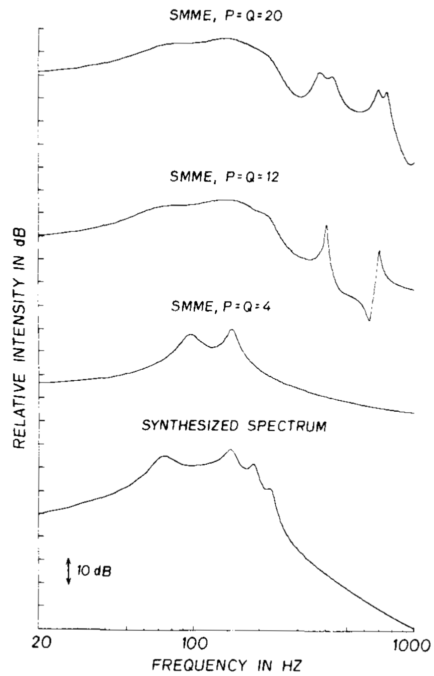

Fig. 4. Comparison of a synthesized mitral sound spectrum with the spectra estimated with the Steiglitz–McBride method (SMME) for P (number of poles) and Q (number of zeros) = 4, 12, and 20. The pole-zero spectra were computed after truncating the synthesized sound by 6 percent of their energy and after adding −35 dB of random noise.

The bias and variability of the spectral parameters estimated with SMME are presented in Table II for P and Q varying from 4 to 20. Except for $Q1$, the bias and variability of the spectral parameters did not improve as P and Q were increased. On the other hand, the bias and variability of $F2$, F-20, RIA20, and BW3 worsen as P and Q are increased to 20. Increasing P and Q has a par-

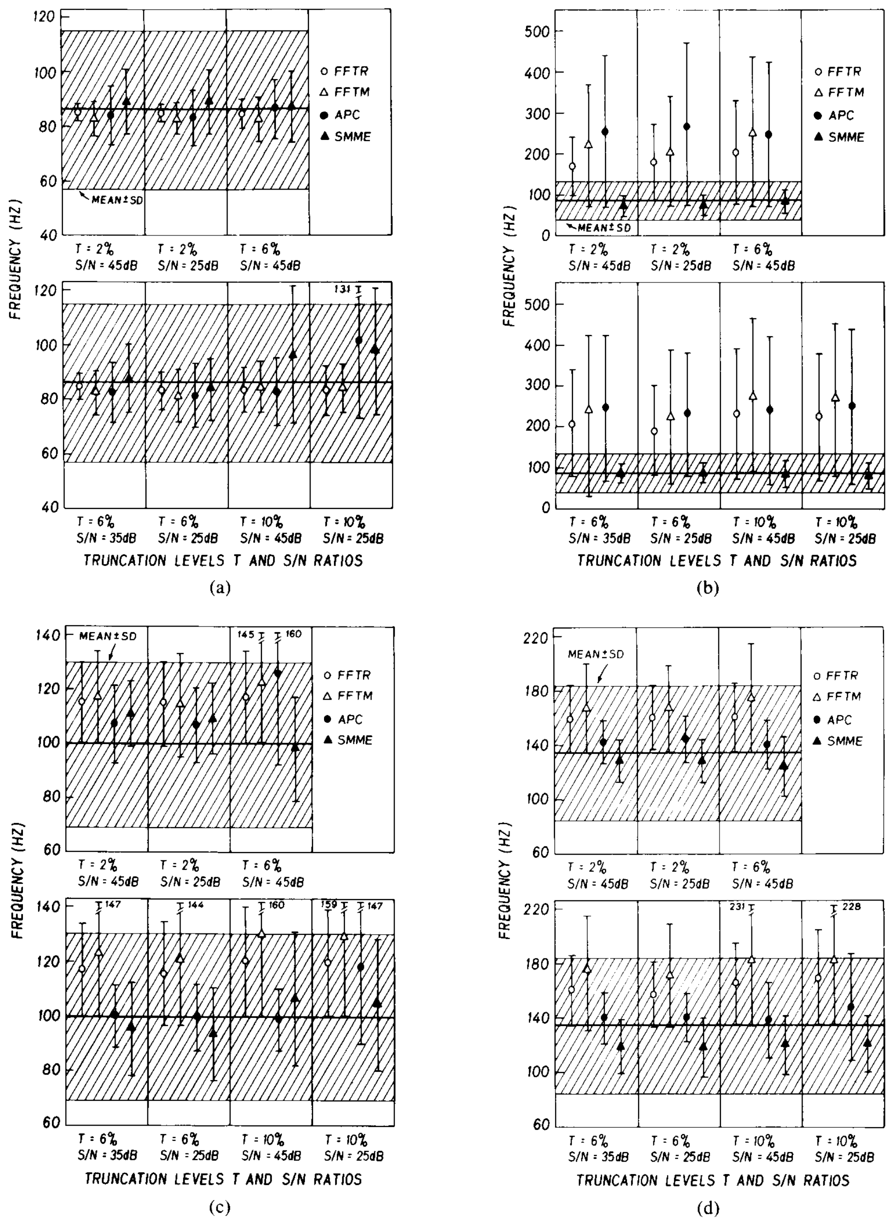

Fig. 5. Bias and variability of $F1$ (a), $F2$ (b), F-3 (c), and F-10 (d) for the FFTR, FFTM, SMME, and APC algorithms following truncation of the mitral sounds and addition of random noise. The mean ± SD range of the reference parameter are represented, respectively, by the horizontal line and the shaded zone.

ticularly strong effect on $F2$ and F-20. With four poles and four zeros, the bias and variability of $F2$ and F-20 were, respectively, -2.5 and 25.2 Hz, and -9.2 and 24.0 Hz. With 20 poles and 20 zeros, the bias and variability of $F2$ increased to 82.7 and 97.5 Hz, and that of F-20 to 123.1 and 140.7 Hz, respectively.

An example of a synthesized spectrum of $M1$ and the corresponding SMME spectra computed for P and Q = 4, 12, and 20 is shown in Fig. 4. Spurious peaks in the high frequency range (above 300 Hz) and a broadening of the dominant spectral peak are observed for P and Q = 12 and 20. The number of false spectral peaks increased with higher P and Q values.

The poor results obtained by using high values of P and Q for SMME are clearly demonstrated in Table II and in Fig. 4. The optimal number of poles and zeros for SMME was then chosen to be four because these values provided the lowest bias and variability of five parameters ($F1$, $F2$, F-20, RIA20, and BW3). Values of P and Q lower than four were evaluated and resulted in oversmoothed

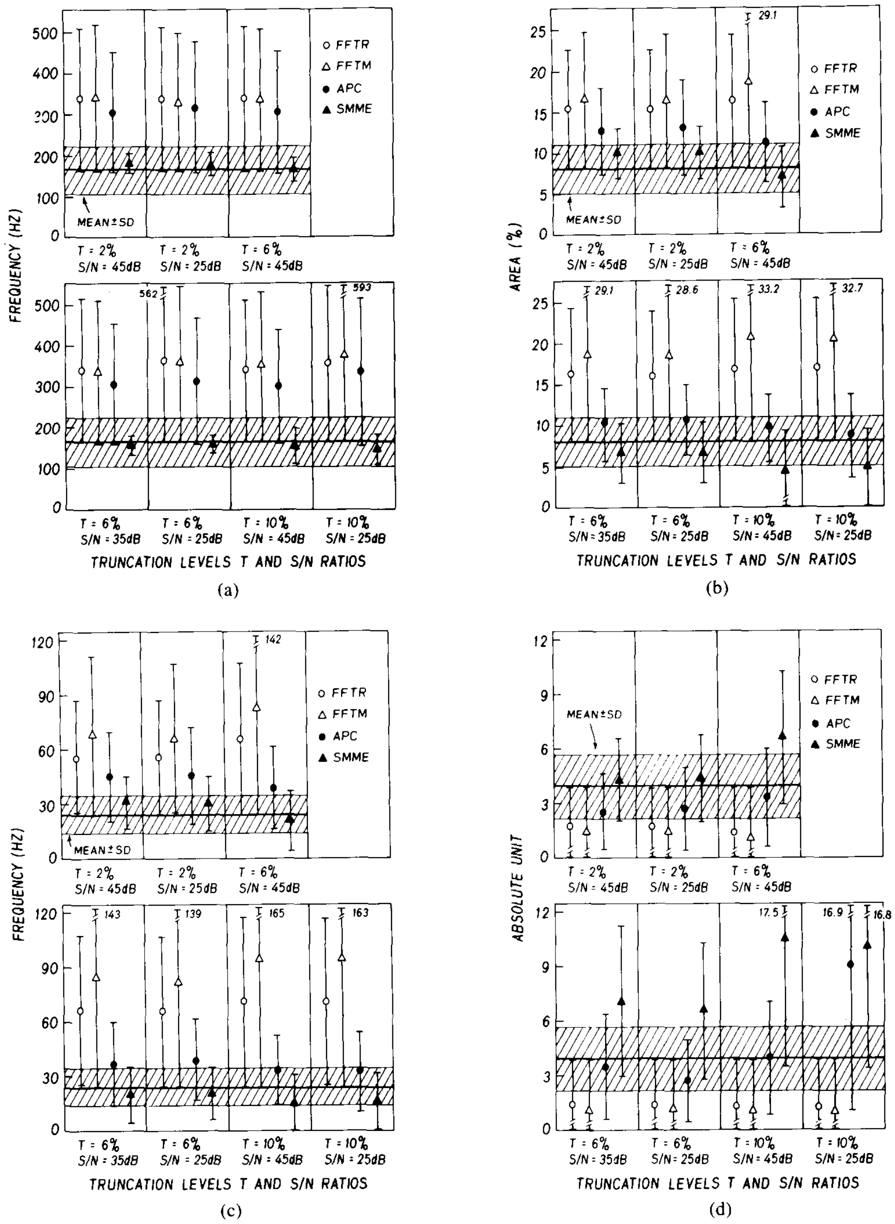

Fig. 6. Bias and variability of F-20 (a), RIA20 (b), BW3 (c), and $Q1$ (d) for the FFTR, FFTM, SMME, and APC algorithms following truncation of the mitral sounds and addition of random noise. The mean $\pm$ SD range of the reference parameter are represented, respectively, by the horizontal line and the shaded zone.

spectra with no second dominant spectral peak. In addition, we also observed an increase of the bias and variability of F-10, F-20, RIA20, and $Q1$ when using two or three poles and zeros. Other combinations of P and Q were not tested.

C. Bias and Variability of the Spectral Parameters

The results on the bias and variability of the spectral parameters are shown in Figs. 5 and 6. Seven combinations of truncation levels and SNR's were used to test the accuracy of the algorithms. The horizontal line on these figures represents the mean value of the spectral parameter extracted from the 19 synthesized reference spectra, uncontaminated by truncation and random noise. The shaded zone indicates the standard deviation (SD) of the parameter. The bias of each diagnostic spectral parameter is proportional to the distance between the mean value estimated with a given algorithm and the horizontal line. The variability in the spectral parameter is proportional to the range of the vertical deviations.

The bias and variability of $F1$ are shown in Fig. 5(a). Except for SMME when the synthesized sounds were truncated by 10 percent and for APC for a truncation level of 10 percent and a SNR of 25 dB, all algorithms provide good estimates of $F1$. However, the fast Fourier transform with rectangular window is the best technique to minimize the variability of $F1$ for all truncation levels and SNR's. As shown in Fig. 5(a), this algorithm also presents the lowest bias value. As shown in Fig. 5(b), only SMME should be used to estimate the second dominant spectral peak of normal mitral heart sounds. It is interesting to note that the variability of $F2$ estimated with SMME increases rather slowly with the perturbation level.

The bias and variability of F-3 and F-10 are shown in Fig. 5(c) and (d), respectively. Except for truncation levels and SNR's of 6 percent and 45 dB, and 10 percent and 25 dB, APC is the best technique to minimize the bias of F-3. This algorithm also minimizes the variability of F-3 for truncation levels and SNR's of 6 percent and 35 dB, 6 percent and 25 dB, and 10 percent and 45 dB. Although APC presents a high bias and variability for two truncation levels and SNR's (6 percent and 45 dB, and 10 percent and 25 dB), this algorithm should be preferred when estimating F-3.

APC and SMME are the best techniques to estimate F-10. APC minimizes both bias and variability for a truncation level of 2 percent. On the other hand, SMME results in minimal bias and variability for a truncation level of 6 percent. For a truncation level of 10 percent, APC reduces the bias and SMME minimizes the variability. Both spectral techniques can thus be used to estimate F-10.

Similarly to $F2$, only SMME should be used to estimate F-20, as shown in Fig. 6(a). Generally, the bias of F-20 increases with higher truncation levels and SNR's. Fig. 6(b) and (c) show the results obtained for RIA20 and BW3. Except for a truncation level of 10 percent, SMME minimizes both bias and variability of RIA20. This algorithm also minimizes bias and variability of BW3 for all truncation levels and SNR's. SMME should then be preferred for estimating RIA20 and BW3.

The bias and variability of $Q1$ are shown in Fig. 6(d). FFTR minimizes the variability of $Q1$ for all truncation levels and SNR's. Except for a truncation level of 10 percent and a SNR of 25 dB, APC, and SMME alternatively minimize the bias of $Q1$. Because the variabilities of APC and SMME are high compared to the values obtain with FFTR, for truncation levels of 6 and 10 percent, FFTR is recommended to estimate $Q1$. However, as seen in Fig. 6(d), the variability of $Q1$ estimated with FFTR is in the same range as the mean value estimated from the synthesized spectra. Although this technique minimizes the variability of $Q1$, the diagnostic use of this parameter is questionable.

D. *Minimum Threshold of the Bias and Variability of the Spectral Parameters*

According to the results reported in Figs. 5 and 6, the use of an optimal spectral technique for each parameter is recommended. Table III shows the minimum values of the bias and variability of the parameters for the truncation level and SNR of the normal mitral acoustic signatures (6 percent and 35 dB). The results presented in this table are those obtained with the spectral algorithm that minimized the bias and variability of each parameter.

TABLE III
BIAS AND VARIABILITY OF EIGHT DIAGNOSTIC SPECTRAL PARAMETERS ESTIMATED FOR THE TRUNCATION LEVEL AND SNR OF THE NORMAL MITRAL ACOUSTIC SIGNATURES (6 PERCENT AND 35 dB) AND OBTAINED WITH THE ALGORITHM THAT MINIMIZED THE BIAS AND VARIABILITY VALUES

PARAMETER (ALGORITHM)	BIAS	VARIABILITY
F1 (FFTR)	-1.4 Hz	5.0 Hz
F2 (SMME)	-2.5 Hz	25.2 Hz
F-3 (APC)	0.4 Hz	11.6 Hz
F-10 (APC)	5.0 Hz	19.2 Hz
F-20 (SMME)	-9.2 Hz	24.0 Hz
RIA20 (SMME)	-1.5 %	3.7 %
BW3 (SMME)	-4.5 Hz	15.5 Hz
Q1 (FFTR)	-1.4	1.4

IV. DISCUSSION

A. *Truncation Level and SNR of the Mitral Sounds*

The truncation level and SNR of normal mitral valve signatures were estimated respectively from the synthesized sounds and from the PCG segments of 19 patients. The absence of significant diastolic acoustic activity was assumed in the estimation of the SNR of normal mitral heart sounds. Diastolic murmurs may be found in patients with aortic regurgitation, mitral stenosis, or tricuspid stenosis [2]. However, none of the patients used in our data base had these pathologies. It was also reported that the diastolic fourth heart sound of the PCG may be heard at the apex [2]. This sound which follows the onset of the P wave of the electrocardiogram by approximately 70 ms [28] was excluded from the diastolic PCG segments used to compute the background noise of the mitral heart sounds. Only the first M samples (where M represents the number of samples in the selected mitral heart sound) of the 200 ms PCG segment preceding $S1$ were used to compute the SNR.

In the present study, the synthesized mitral sounds were perturbed by truncating them by 2, 6, and 10 percent of their total energy, and by adding -45, -35, and -25 dB of random noise. These values were chosen specifically to match those observed on the real acoustic mitral signatures.

B. *Number of Poles and Zeros for SMME and APC Algorithms*

The number of poles (P) and zeros (Q) used in parametric methods is very important in the assessment of the spectral characteristics. A low-order model produces a smoothed spectrum with low-frequency resolution, whereas a high order model introduces spurious peaks and details for maximum entropy spectral analysis [16], [22], [26]. In this paper, the presence of false spectral peaks for high order models was clearly demonstrated in Fig. 4 for the Steiglitz–McBride method with maximum entropy. However, the use of a low-order model did not clearly show a reduction in frequency resolution. Indeed, as shown on Table II, the minimum bias and variability for the two most dominant spectral peaks were obtained with a model using four poles and four zeros. In addition, increasing the values of P and Q did not improve the resolution of the third and fourth spectral peaks of the synthesized reference spectrum shown in Fig. 4.

To prevent oversmoothing or production of false spectral peaks, we have proposed to select P and Q where the plateau of the NRMSE function begins [21]. Using this criterion, 16 poles were found to be optimal for estimating mitral heart sound spectra with the all-pole modeling and covariance method. This value of P was also shown to minimize variability of six spectral parameters. This criterion did not however perform well with SMME. As shown on Table II, lower bias and variability of the parameters were obtained by using four poles and four zeros instead of 20 poles and 20 zeros.

Our criterion was based on the work of Childers [22] and Joo [23]. Childers [22] proposed the calculation of the mean-square error between the modeled signal and the impulse response of the all-pole model, for different values of P. When the error suddenly decreases by a significant step, this value of P was suggested as optimal. A different criterion was proposed by Joo [23] for pole-zero modeling of valve closing sounds. Essentially, it consists in comparing the signal to the impulse response of the model as P and Q are varied and to select the combination that provides the minimum error. According to the results presented here, our criterion was good for all-pole modeling but not very useful for pole-zero modeling. Even if this criterion is optimal for modeling the signal, it does not allow the minimization of the bias and variability of the parameters selected from the pole-zero spectral estimates. This is mainly due to the presence of false spectral peaks.

C. Bias and Variability of the Spectral Parameters

Additional information is given here concerning the results shown in Figs. 5 and 6. All bias and variability measurements were averaged for the 19 patients. Parameter $F2$ could only be extracted from 15 of the 19 synthesized spectra. In addition, each algorithm extracted a different number of $F2$ peaks. For instance, FFTR and FFTM tend to extract $F2$ even when it is missing. $F2$ was observed on most FFTR spectra for all truncation levels and SNR's. Between 16 and 18 $F2$ peaks were extracted with FFTM. The number of spectra with a second dominant peak tends to decrease with increasing truncation level. The best algorithm for detecting $F2$, for all truncation levels and SNR's is APC. An average of 15.4 $F2$ peaks (range of 14–17) were detected with this algorithm. Finally, as with FFTM, the number of SMME spectra with a second dominant peak tends to decrease with increasing truncation level. For truncation levels of 2, 6, and 10 percent, the average number of detected $F2$ were, respectively, 18, 14.3, and 11.

V. Conclusion

The power spectra of 19 synthesized mitral acoustic signatures were used as standard to compare four algorithms (FFTR, FFTM, APC, and SMME) in extracting eight diagnostic spectral parameters. Because of the high correlation (99 percent) and low NRMSE (14 percent) found between the mitral acoustic signatures and the synthesized sounds, it is estimated that the synthesized reference power spectra correspond well to the theoretical spectra of normal mitral heart sounds and can thus be termed as "reliable standard."

Bias and variability of diagnostic spectral parameters were presented in this paper for different truncation levels and SNR's of normal mitral heart sounds. An important finding of this paper is that no single spectral estimation algorithm is ideal for extracting all eight parameters. For instance, the fast Fourier transform with rectangular window should be used for $F1$ and $Q1$, the Steiglitz–McBride method with maximum entropy (four poles and four zeros) for $F2$, F-20, RIA20, and BW3, the all-pole modeling with covariance method (16 poles) for F-3, and either APC or SMME for F-10. If the same method must be used to extract the eight parameters, SMME is recommended because this technique minimizes the bias and variability of five of them.

The worse results concerning the extraction of the spectral parameters were obtained by using the fast Fourier transform with Hamming window. The fast Fourier transform with rectangular window also performed badly for extracting parameters $F2$, F-3, F-10, F-20, RIA20, and BW3. Generally, the parametric spectral techniques were superior to the FFT-based techniques. However, bias and variability similar to that of the FFT-based techniques were obtained with APC for extracting $F2$ and F-20. Except for $Q1$, SMME always gave consistent results.

In a previous paper [13], accuracy of diagnostic spectral parameters extracted from normal aortic heart valves were presented. Eight techniques were tested and for each of them, three parameters were extracted. These were $F1$, $F2$, and the bandwidth at -30 dB of the spectrum. FFTR was the best technique to estimate $F1$. Bias and variability of 4.0 and 10.0 Hz were obtained for the truncation level and SNR of normal aortic heart sounds (8 percent and 40 dB). In this paper, bias and variability of -1.4 and 5.0 Hz were reported when $F1$ was extracted with FFTR. This confirms the stability of this method for extracting $F1$.

Similarly, SMME was also the best technique to estimate $F2$ of normal aortic heart sounds [13]. Bias and variability of 22.0 and 50.0 Hz were reported. These high bias and variability, compared to the values of -2.5 and 25.2 Hz reported here, can be explained by the different values of P and Q used in the previous study (14 poles and 14 zeros). These values were computed from the NRMSE function but were not validated to confirm if they minimized the bias and variability of $F2$. Better results could probably have been obtained by using lower values of P and Q.

In conclusion, the results presented in this paper provide new information for improving the performance of pattern recognition techniques based on the extraction of spectral diagnostic features from the valve closing sound spectra. Better discrimination between normal and degenerated bioprosthetic valves, implanted in the mitral position, should be obtained by using the optimal spectral algorithm for each diagnostic parameter.

Acknowledgment

The authors gratefully acknowledge the contributions of the following persons: Dr. M. Brais of the University of Ottawa Heart Institute and Civic Hospital for selecting the patient population, F. Durand for performing the data acquisition and synthesis of the mitral valve closing sounds, M.-C. Grenier for computing the SNR of the mitral sounds, A. Chénier and M. Blanchard for technical assistance, and I. Morin for preparing the illustrations.

References

[1] J. A. Shaver, R. Salerni, and P. S. Reddy, "Normal and abnormal heart sounds in cardiac diagnosis. Part I: Systolic sounds," *Curr. Probl. Cardiol.*, vol. 10, pp. 1-69, Mar. 1985.

[2] A. G. Tilkian and M. Boudreau Conover, *Understanding Heart Sounds and Murmurs with an Introduction to Lung Sounds*, 2nd ed. Toronto, Canada: W. B. Saunders, 1984.

[3] A. Leatham, *Auscultation of the Heart and Phonocardiography*, 2nd ed. New York: Churchill Livingstone, 1975.

[4] M. E. Tavel, *Clinical Phonocardiography and External Pulse Recording*, 2nd ed. Chicago, IL: Year Book Medical, 1976.

[5] A. A. Luisada, L. Frazin, A. Singhal, and A. Nunez, "Various types of systolic clicks in patients with muscular subaortic stenosis," *Japan Heart J.*, vol. 26, pp. 133-143, Jan. 1985.

[6] R. L. Szkopiec, K. B. Desser, A. Benchimol, and C. Sheasby, "Phonocardiographic findings in patients with normally functioning Ionescu-Shiley prostheses," *Amer. J. Cardiol.*, vol. 51, pp. 969-972, Mar. 1983.

[7] G. Cloutier, M. C. Grenier, R. Guardo, and L. G. Durand, "Spectral analysis of closing sounds produced by Ionescu-Shiley bioprosthetic aortic heart valves. Part II: Computer simulation of aortic closing sounds and estimation of their truncation level and signal-to-noise ratio," *Med. Biol. Eng. Comput.*, vol. 25, pp. 492-496, Sept. 1987.

[8] L. G. Durand, J. de Guise, G. Cloutier, R. Guardo, and M. Brais, "Evaluation of FFT-based and modern parametric methods for the spectral analysis of bioprosthetic valve sounds," *IEEE Trans. Biomed. Eng.*, vol. BME-33, pp. 572-578, June 1986.

[9] P. D. Stein, H. N. Sabbah, J. B. Lakier, D. J. Magilligan, Jr., and S. Goldstein, "Frequency of the first heart sound in the assessment of stiffening of mitral bioprosthetic valves," *Circulation*, vol. 63, pp. 200-203, Jan. 1981.

[10] P. D. Stein, H. N. Sabbah, J. B. Lakier, S. R. Kemp, and D. J. Magilligan, Jr., "Frequency spectra of the first heart sound and of the aortic component of the second heart sound in patients with degenerated porcine bioprosthetic valves," *Amer. J. Cardiol.*, vol. 53, pp. 557-561, Feb. 1984.

[11] L. G. Durand, M. Blanchard, H. N. Sabbah, M. S. Hamid, S. R. Kemp, and P. D. Stein, "A Bayes model for automatic detection and quantification of bioprosthetic valve degeneration," *Math. Comput. Modeling*, vol. 11, pp. 158-163, 1988.

[12] P. J. Arnott, G. W. Pfeiffer, and M. E. Tavel, "Spectral analysis of heart sounds: Relationships between some physical characteristics and frequency spectra of first and second heart sounds in normals and hypertensives," *J. Biomed. Eng.*, vol. 6, pp. 121-128, Apr. 1984.

[13] G. Cloutier, R. Guardo, and L. G. Durand, "Spectral analysis of closing sounds produced by Ionescu-Shiley bioprosthetic aortic heart valves. Part III: Performance of FFT-based and parametric methods for extracting diagnostic spectral parameters," *Med. Biol. Eng. Comput.*, vol. 25, pp. 497-503, Sept. 1987.

[14] G. Cloutier, L. G. Durand, M. C. Grenier, R. Guardo, and M. Brais, "Computer simulations of acoustic closing sounds produced by bioprosthetic heart valves," in *Proc. IEEE Computer Cardiol.*, Linkoping, Sweden, Sept. 1985, pp. 243-246.

[15] H. Koymen, B. K. Altay, and Y. Z. Ider, "A study of prosthetic heart valve sounds," *IEEE Trans. Biomed. Eng.*, vol. BME-34, pp. 853-863, Nov. 1987.

[16] S. M. Kay and S. L. Marple, Jr., "Spectrum analysis: A modern perspective," *Proc. IEEE*, vol. 69, pp. 1380-1419, Nov. 1981.

[17] K. Steiglitz and L. E. McBride, "Technique for the identification of linear systems," *IEEE Trans. Automat. Contr.*, vol. AC-10, pp. 161-164, Oct. 1965.

[18] K. Steiglitz, "On the simultaneous estimation of poles and zeros in speech analysis," *IEEE Trans. Acoust., Speech, Signal Processing*, vol. ASSP-25, pp. 229-234, June 1977.

[19] A. H. Gray, Jr., and J. D. Markel, "Linear prediction analysis programs (Auto-Covar)," in *Programs for Digital Signal Processing*, IEEE Acoustics, Speech, and Signal Processing Society, New York: Wiley 1979, pp. 4.1-1-4.1-7.

[20] J. Makhoul, "Linear prediction: A tutorial review," *Proc. IEEE*, vol. 63, pp. 561-580, Apr. 1975.

[21] G. Cloutier, R. Guardo, and L. G. Durand, "Spectral analysis of closing sounds produced by Ionescu-Shiley bioprosthetic aortic heart valves. Part I: Optimal number of poles and zeros for parametric spectral analysis," *Med. Biol. Eng. Comput.*, vol. 25, pp. 487-491, Sept. 1987.

[22] D. G. Childers, "Modern spectral analysis," in *Proc. IEEE Frontiers Eng. Health Care*, Colorado, Oct. 1979, pp. 104-109.

[23] T. H. Joo, "Pole-zero modeling and classification of phonocardiograms," Master's thesis, Massachusetts Institute of Technology, Cambridge, MA, Jan. 1982.

[24] H. Akaike, "Statistical predictor identification," *Ann. Inst. Stat. Math.*, vol. 22, pp. 203-217, 1970.

[25] H. Akaike, "A new look at the statistical model identification," *IEEE Trans. Automat Contr.*, vol. AC-19, pp. 716-723, Dec. 1974.

[26] B. V. K. Vijaya Kumar and S. K. Mullick, "Power spectrum estimation using maximum entropy method," *J. Inst. Electron. Telecomm. Eng.*, vol. 25, pp. 181-194, May 1979.

[27] S. W. Lang and J. H. McClellan, "Frequency estimation with maximum entropy spectral estimators," *IEEE Trans. Acoust., Speech Signal Processing*, vol. ASSP-28, pp. 716-724, Dec. 1980.

[28] P. S. Reddy, R. Salerni, and J. A. Shaver, "Normal and abnormal heart sounds in cardiac diagnosis. Part II: Diastolic sounds," *Curr. Probl. Cardiol.*, vol. 10, pp. 1-55, Apr. 1985.

Guy Cloutier (S'89) was born in Trois-Rivières, Québec, Canada, in 1961. He received the B.Eng. degree in electrical engineering from the Université du Québec à Trois-Rivières in 1984 and the M.Sc.A degree in biomedical engineering from the Ecole Polytechnique, University of Montreal in 1986. He is now completing the Ph.D. degree in biomedical engineering at the Ecole Polytechnique and the Clinical Research Institute of Montreal.

In 1982 and 1983, he received the University Undergraduate Student Research Awards from the Natural Sciences and Engineering Research Council of Canada (NSERC). Since 1984 he has received Postgraduate Scholarships from NSERC, the Fonds de la Recherche en Santé du Québec, and the Fonds pour la Formation de Chercheurs et l'Aide à la Recherche. His principal research interests of his are digital signal processing and pattern recognition applied to echo-Doppler and phonocardiographic signals.

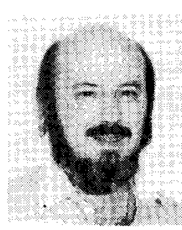

Louis-Gilles Durand (M'78–SM'85) received the B.S., M.S. and Ph.D. degrees in electrical engineering from the Ecole Polytechnique, University of Montreal, Montreal, Quebec, Canada, in 1975, 1979, and 1983, respectively.

He joined the Clinical Research Institute of Montreal in 1975 to set up a Service of Biomedical Engineering while continuing his postgraduate studies. He is presently the Director of the Biomedical Engineering Laboratory and Director of the Department of Specialized Equipment at the

Clinical Research Institute of Montreal. He is also a Research Assistant Professor in the Department of Medicine at the University of Montreal and a Visiting Professor at the Institute of Biomedical Engineering of the Ecole Polytechnique. His major interests are digital signal processing of physiological signals, computer modeling of physiological systems, image processing, and medical instrumentation.

Robert Guardo was born in Siracusa, Italy, in 1946. He received the B.Sc. degree in engineering physics from the Ecole Polytechnique, Montreal, Canada, in 1968 and the Ph.D. degree in electrical engineering from Imperial College, London, England, in 1972.

From 1972 to 1973 he was a Research Associate at the Neurosurgery Clinic of the University of Dusseldorf, West Germany. He then joined the Biomedical Engineering Institute of the Ecole Polytechnique, University of Montreal, where he is currently Full Professor. His major interests are cardiac electrophysiology and haemodynamics, digital signal processing, and instrumentation design.

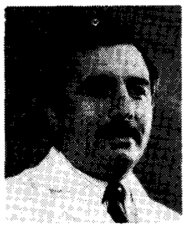

Hani N. Sabbah received the B.S. degree in aerospace engineering in 1972 from the University of Oklahoma, Norman. He is now completing the Ph.D. degree in biomedical sciences-medical physics at Oakland University, Rochester, MI.

He is currently an Assistant Staff Investigator in cardiovascular research at the Henry Ford Heart and Vascular Institute, Detroit, MI. His principal research interests are ventricular function/coronary circulation and the role of fluid dynamics in artherogenesis.

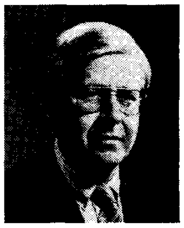

Paul D. Stein received the B.S. degree in physics in 1955 and the M.D. degree in 1959, both from the University of Cincinnati, Cincinnati, OH.

After internship and residency in internal medicine, he took fellowship training in cardiology at the University of Cincinnati, Mount Sinai Hospital, NY, and Harvard Medical School, Boston, MA. He was on the faculty of the University of Oklahoma, Norman, from 1969 to 1976 as a Professor of Research Medicine. From 1976 to the present time, he has been at Henry Ford Hospital, Detroit, MI, where he is Director of Cardiovascular Research. He is also Adjunct Professor of Physics at Oakland University, Rochester, MI.